

A hybrid-wavelet artificial neural network model for monthly water table depth prediction

Anandakumar^{1,*}, A. R. Senthil Kumar², Ravindra Kale³, B. Maheshwara Babu¹, U. Sathishkumar¹, G. V. Srinivasa Reddy¹ and Prasad S. Kulkarni¹

¹Department of Soil and Water Engineering, College of Agricultural Engineering, Raichur 584 104, India

²National Institute of Hydrology, Roorkee 247 667, India

³Western Himalayan Regional Centre, National Institute of Hydrology, Jammu 180 003, India

Groundwater is an essential natural resource in the country to fulfil the irrigation, domestic, industrial and other needs. In order to ensure sustainable use of groundwater resources, the groundwater level is used as an important indicator for balancing the groundwater withdrawal rate and replenishment rate through the recharge. Quantitatively, the recharge rate is governed by various complex large-scale hydrological processes and hence achievement of sustainability of groundwater supplies, through sustainable withdrawal rate is a complicated issue. In the present study, a data-driven prediction model by combining discrete wavelet transform (DWT) with artificial neural network (ANN) called as wavelet artificial neural network (WANN) is proposed for the groundwater table prediction. The simulation results obtained by regular ANN model were compared with those obtained by WANN model to prove the superiority of the latter model over the former. WANN model was developed using decomposed signals of rainfall, evapotranspiration and water table depth time series as inputs in the ANN model to arrive at a prediction of monthly fluctuation of the groundwater table. Rainfall time series was decomposed using Haar wavelet at third decomposition level and evapotranspiration and water table depth time series was decomposed using Daubechies wavelet at second decomposition level. The RMSE value of ANN and WANN model during validation were found to be 0.3648 m and 0.1695 m respectively, which showed decrease in RMSE value by 0.195 m when WANN was applied. Model efficiencies of ANN and WANN model during validation were 84.65% and 95.68%, indicating excellent improvement of model accuracy after applying WANN. Hence, the proposed WANN model seems to be a promising tool to predict the monthly water table fluctuation.

Keywords: Artificial neural network, wavelet transformation, wavelet artificial neural network, water table depth prediction.

In the arid and semiarid regions where surface water resources are limited due to a low degree of precipitation

and a high degree of evapotranspiration, groundwater is utilized to fulfil the various water requirements. In India, the current groundwater use rate exceeds above 65% for irrigation and 85% for drinking water supplies in rural and urban areas. Since the last decade, the groundwater management is becoming a critical issue due to increased water demand, reduced rainfall, drought and consequently water shortages in the country. Efficient management of groundwater resource needs a clear understanding of the effects of climate variability as well as anthropogenic activities on groundwater level recharge, particularly in the perspective of increasing climate uncertainty. Accurate groundwater table depth prediction is necessary to understand the regional groundwater status well in advance for sustainable planning and management of the available water resource.

In the recent past, computational intelligence techniques like artificial intelligence, artificial neural network, fuzzy logic and genetic algorithm models are being used intensively to simulate the most uncertain hydrological processes due to their enhanced performance over the traditional modelling techniques, viz. empirical models, statistical models like autoregressive, autoregressive moving average models and physical-based models which are data-intensive and time consuming. Artificial neural network (ANN) has gained warm response as a new promising alternative in this field. ANN model is treated as universal approximator, also its strength lies in capturing the input and output relation of the process without enough knowledge of the underlying principles. The advantages and suitability of ANN models have been described elsewhere¹. Neural networks have previously been applied for groundwater level prediction²⁻⁵.

ANN is widely accepted, applicable and considered as a flexible tool for modelling of hydrological processes. ANN has also some limitations when applied to a high non-stationary signal involving seasonality varying from 1 day to several decades. Hence, pre-processing of time and space data may be considered as an effective method to overcome these drawbacks. In recent years, wavelet transformation technique is emerging as an efficient tool for preprocessing of data series.

The observed time series would exhibit non-stationary characteristics, which is a significant challenge for several

*For correspondence. (e-mail: anandk624@gmail.com)

fields (e.g. remote sensing, engineering, hydrology, etc.). The wavelet transform has been extensively studied in several applications related to climate, meteorology, oceanography, geosciences and geophysics. In order to decompose the non-stationary time series into time-frequency domain, wavelet transform (WT) has been successfully applied over different range of fields⁶. The wavelet transform is the improved version of Fourier transform. Fourier transform is a powerful tool for analysing the components of a stationary signal, but it cannot be applied for analysing the components of a non-stationary signal. Whereas, the wavelet transform is advantageous over Fourier transform as it can be applied to analyse the components of a non-stationary signal. Effectiveness of the wavelet transform in disintegrating non-stationary time series into a number of stationary signals at different scales (levels) is helpful for better understanding of the process. Therefore, a role of data-driven prediction model by combining wavelet transform with ANN known as the wavelet-ANN (WANN) model is inevitable as it can explain concurrently spatial and temporal information of the time series, produces an effective implementations for prediction of hydrological processes with improved prediction accuracy^{7,8}. Since its theoretical development in 1984, the wavelet transform has attracted significant attention⁹. A number of recent hydrological modelling studies have implemented wavelet analysis¹⁰⁻¹⁷.

Materials and methods

Study area

The data from a groundwater monitoring station located at the hydro-meteorological observatory at the National Institute of Hydrology (NIH) campus, Roorkee was selected for this study. Daily rainfall, water table depth and maximum, minimum and mean temperature data of Roorkee station were collected from July 2008 to April 2013. Evapotranspiration was calculated using Hargreaves temperature model (eq. (1))

$$ET = 0.0023R (T_{mean} + 17.8) (T_{max} - T_{min})^{1/2}, \tag{1}$$

where ET is evapotranspiration in (mm/day), T_{mean} , T_{max} and T_{min} is mean, maximum and minimum air temperatures (°C) respectively, and R is extraterrestrial radiation (mm/day)¹⁸.

Hybrid wavelet ANN model development

Development of hybrid wavelet ANN model involves the development of ANN model using pre-processed (decomposed) time series of all the desired variables using wavelet transformation as the input to the model. The hybrid model helps in understanding the combined applica-

tion of the ANN method with the wavelet transform to improve the performance of the model significantly.

Basically, ANN is categorized based on its network architecture representing the connection pattern between nodes, method of determining the weights of the connection and activation function used¹⁹. In this study, feed-forward neural network architecture was used in predicting monthly water table depths. The selection of significant input variables is one of the most important steps in ANN modelling. Generally, all the possible input variables are not equally informative, because some input variables may be correlated, noisy, or may not have any correlation with the output variable²⁰. Hence, statistical methods like cross-correlation, auto-correlation and partial auto-correlation techniques were used to select the significant input variables.

Feed-forward neural network

Feed-forward means that all the interconnections between input, hidden and output layers propagate in the forward direction to the next layer, and flow of information is only in the forward direction. Each node from the one layer is interconnected to the next layers. These interconnections are assigned with weights based on the influence of each input parameters to the output. In ANN, the type of node used determines the method in which it calculates the total input and the method in which the node calculates its output as a function of its net input (eq. (2)). Each node in ANN operates as processing elements that react to the weighted inputs received from other or from previous nodes as shown in Figure 1.

The net input x_j to node j is the weighted sum of all the incoming signals as given in eq. (2).

$$\text{net input} = x_j = \sum w_{ij}y_i, \tag{2}$$

where x_j is the net input coming to node j ; w_{ij} the weight between node i and node j ; y_i is the activation function at node i .

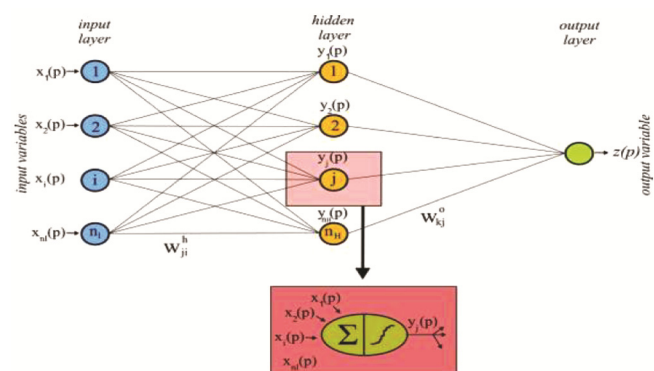


Figure 1. A typical representation of the feed-forward neural network.

The log sigmoidal activation function as given by eq. (3), was used between input and the hidden layers

$$y_i = 1/[1 + \exp(-x_j)]. \quad (3)$$

Typical feed-forward neural network with input–output combinations is presented in Figure 1. The feed-forward neural network is easy to handle, and can approximate any input–output mapping. However, training of the network is time-consuming and requires lot of training data.

Training with algorithm

Determining the best values of all weights and updating the weights to reduce the error in time series prediction is called training of ANN. Weights are usually randomly set in the initial iterations, which are then adjusted so that the next iteration will produce near value between the desired and the actual output. The training phase can consume a lot of time. In the present study, Bayesian regularization algorithm was used to train the network more efficiently. This algorithm will automatically set optimum values for the parameters of the objective function. The weights and biases of the network were assumed to be random variables with specified distributions. The main advantage of this algorithm is that the function will not be over-fitted even for the large size of the network. Bayesian regularization was successfully used in many studies^{21,22}.

Network architecture

The number of neurons in the hidden layer was identified by trial and error method. The network was trained for each set of hidden neurons with the input datasets in batch mode to minimize the error and to enhance the performance of the model at the output layer. Various internal parameters used in the ANN model like learning rate, momentum coefficient, scalar μ (momentum parameter), and combination of transfer functions for hidden and output layer were also found out by trial and error. MATLAB 2012a software was used for this analysis.

Wavelet transformation

Wavelet is a ‘small wave’ having a finite length in space. It is a special kind of function which exhibits oscillatory behaviour for a short period of time and then dies out. The wavelet function, $\varphi(t)$, signifying the time-frequency localization is given by eq. (4)

$$\varphi_{\tau,s}(t) = [1/s^{1/2}]\varphi[t - \tau/s]. \quad (4)$$

where s (>0) indicates the scaling parameter and τ indicates the translation parameter. For the function to be a wavelet, it should be time-limited. For a given scaling

parameter s , the wavelet is translated by varying the parameter τ .

Wavelets are short duration finite energy functions. They transform the signal under analysis into another illustration which presents the signal in a more detailed form. This transformation of the signal is called a wavelet transform. In wavelet transform, a single function, called the mother wavelet, is dilated and translated to obtain a set of ortho-normal basis functions.

There are two methods in wavelet transformation, viz. continuous wavelet transform (CWT) represented in eq. (5) and discrete wavelet transform (DWT).

$$\text{CWT}_{\tau,s} = \frac{1}{\sqrt{s}} \int f(t)\varphi[t - \tau/s]dt. \quad (5)$$

The CWT is obtained after continuous shifting of the wavelet along the signal. In contrast, the discrete wavelet transformation obtained after shifting the wavelet in discrete steps, with step-length equal to 2^j ($j = 1, 2, \dots, n$). DWT is computed by successive low-pass and high-pass filtering using Mallat’s algorithm²³. First, the signal ($X[n]$) which is to be transformed is decomposed into high-frequency ($H[n]$), called as detailed coefficient and low-frequency components ($L[n]$), called approximate coefficient. The detailed coefficient ($H[n]$) indicates level 1 coefficient. Then the approximate coefficients ($L[n]$) are once again decomposed into the next level and so on. This splitting carried out using eqs (4), (5) and (6) was called decomposition.

$$X[n] = (x * g)[n] = \sum_{k=-\infty}^{\infty} x[k]g[n-k], \quad (6)$$

$$L[n] = \sum_{k=-\infty}^{\infty} x[k]g[2n-k], \quad (7)$$

$$H[n] = \sum_{k=-\infty}^{\infty} x[k]h[2n-k]. \quad (8)$$

In one-dimensional DWT, the signal is divided into two parts, viz. the high frequency and the low frequency part²⁴. This will enhance the resolution in frequency thus reducing its uncertainty by half. As a result, each filtered band will have band occupancy of $\omega/2$, which can be sampled at ω . The entire signal after the first level of decomposition is represented by only half the number of samples because the decimation by two halves the time resolution. Thus, in the second level of decomposition, the decimation by two doubles the scale while the half-band low-pass filtering removes half of the frequencies. By this method, at high frequencies, the time resolution in the signal gets improved, at low frequencies, the frequency resolution is improved. Such a procedure is repeated until the desired levels of resolution in frequency are attained²⁵. In this study, Haar wavelet and Daubechies

wavelets were used for decomposing the input signal of the time series.

Haar wavelets

The wavelet Haar works on data by calculating the sums and differences of adjacent elements. First it will operate on adjacent horizontal elements and secondly on adjacent vertical elements. The size of the square which contains the most important information is reduced by a factor of 4 after every transform and the translated versions are called ‘mother wavelet’ and represented by $\psi(t)$. The Haar wavelet transformation has several advantages, viz. simple in concept, quick, memory efficient, and precisely reversible without the edge effects that are not possible with other wavelet transforms.

Daubechies wavelets

Discrete wavelet transforms (Daubechies wavelets) are a family of orthogonal wavelets characterized by a maximum number of vanishing moments for some given support. In this type of wavelet, a scaling function (father wavelet) generates an orthogonal multiresolution analysis. This wavelet has intimate connections with the theory of fractals and also has balanced frequency responses. Daubechies wavelets use overlapping windows, so the high-frequency coefficient spectrum reflects all high-frequency changes. Therefore it is useful in noise removal and compression of audio signal processing. Accordingly, the different types of wavelets used in the study are shown in Figure 2.

Performance evaluation criteria

The statistical parameters like coefficient of efficiency as given by eq. (9) and root mean square error as given by eq. (10) were used to check the performance of the models during calibration and validation.

$$CE = \left\{ 1 - \frac{\text{residual variance}}{\text{initial variance}} \right\} = \left\{ 1 - \frac{\sum_{j=1}^n (Y_j - X_j)^2}{\sum_{j=1}^n (Y_j - \bar{Y})^2} \right\}. \quad (9)$$

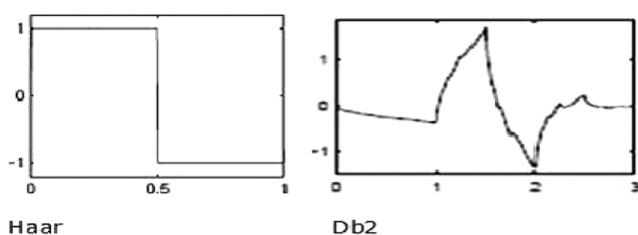


Figure 2. Different type of wavelet (Haar and Daubechies (Db2)).

$$RMSE = \left(\frac{\text{residual variance}}{n} \right)^{1/2} = \left\{ \frac{\sum_{j=1}^n (Y_j - X_j)^2}{n} \right\}^{1/2}, \quad (10)$$

where Y_j is the observed water table depth, X_j the predicted water table depth, n the number of observations, \bar{Y}_j is the mean of observed water table depth.

Results and discussion

The auto-correlation function (ACF), partial auto-correlation function (PACF) and cross-correlation function (CCF) were used to find out significant lags for input variables. The ACF and PACF of water table depth values, the CCF between monthly total evapotranspiration values and monthly mean water table depth values and the CCF between monthly total rainfall values and monthly mean water table depth values were analysed. From the results obtained it can be summarized that the water table depth with one month ($t - 1$) time lag, rainfall with two month ($t - 2$) time lag and ET with one month ($t - 1$) time lag were selected as desired time lags for the proposed model. Based on this output, the final input vector is formulated as

$$H(t) = f \{R(t - 2), ET(t - 1), H(t - 1)\}. \quad (11)$$

Development of WANN model

The input variables, viz. rainfall, evapotranspiration and water level depth time series were decomposed using the wavelet transform at different decomposition levels. The trial and error procedure was adopted to obtain optimum decomposition level. In order to have a comprehensive overview of decomposition level, initially the eq. (12) was employed, which gave minimal decomposition level²⁶.

$$L = \text{int} [\log(N)], \quad (12)$$

where L is the level of decomposition and N is the number data on time series. In this study, the value of data point in time series, $N = 56$ and thus $L = 2$.

This thumb rule equation (eq. (12)) is derived for fully autoregressive signals based on a number of data on time series, and it does not consider the seasonal variations in the data set. Therefore, for the betterment of the model efficiency two additional decomposition levels (i.e. 3 and 5) were also examined, in which decomposition level 2 led to better results. Evapotranspiration and water table depth have a proportionally relative relationship and also have the same seasonality level, so both the signals were decomposed at the same decomposition level (i.e. level 2). The shape of the Daubechies wavelet

Table 1. Results of WANN model during calibration and validation

Model no.	Input combination	WANN structure	Calibration			Validation		
			CORR	RMSE (m)	EFF%	CORR	RMSE (m)	EFF%
WANNGWL1	Haar-3 R (t-2), DB-2 ET (t-1), DB-2H (t-1)	3-1-1	0.9453	0.2674	89.35	0.9739	0.1963	94.22
WANNGWL2	Haar-3 R (t-2), DB-2 ET (t-1), DB-2H (t-1)	3-2-1	0.9662	0.2114	93.35	0.9814	0.1754	95.38
WANNGWL3	Haar-3 R (t-2), DB-2 ET (t-1), DB-2H (t-1)	3-3-1	0.9714	0.1946	94.36	0.9813	0.1698	95.68
WANNGWL4	Haar-3 R (t-2), DB-2 ET (t-1), DB-2H (t-1)	3-4-1	0.9714	0.1946	94.36	0.9813	0.1697	95.68
WANNGWL5	Haar-3 R (t-2), DB-2 ET (t-1), DB-2H (t-1)	3-5-1	0.9714	0.1946	94.36	0.9813	0.1697	95.68
WANNGWL6	Haar-3 R (t-2), DB-2 ET (t-1), DB-2H (t-1)	3-6-1	0.9714	0.1946	94.36	0.9813	0.1697	95.68
WANNGWL7	Haar-3 R (t-2), DB-2 ET (t-1), DB-2H (t-1)	3-7-1	0.9712	0.1955	94.31	0.9804	0.1736	95.48
WANNGWL8	Haar-3 R (t-2), DB-2 ET (t-1), DB-2H (t-1)	3-8-1	0.9714	0.1946	94.36	0.9813	0.1696	95.68
WANNGWL9	Haar-3 R (t-2), DB-2 ET (t-1), DB-2H (t-1)	3-9-1	0.9714	0.1946	94.36	0.9813	0.1697	95.68
WANNGWL10	Haar-3 R (t-2), DB-2 ET (t-1), DB-2H (t-1)	3-10-1	0.9714	0.1946	94.36	0.9813	0.1695	95.68
WANNGWL11	Haar-3 R (t-2), DB-2 ET (t-1), DB-2H (t-1)	3-11-1	0.9714	0.1946	94.36	0.9813	0.1696	95.68
WANNGWL12	Haar-3 R (t-2), DB-2 ET (t-1), DB-2H (t-1)	3-12-1	0.9714	0.1946	94.36	0.9813	0.1696	95.68
WANNGWL13	Haar-3 R (t-2), DB-2 ET (t-1), DB-2H (t-1)	3-13-1	0.9714	0.1946	94.36	0.9813	0.1697	95.68
WANNGWL14	Haar-3 R (t-2), DB-2 ET (t-1), DB-2H (t-1)	3-14-1	0.9713	0.1949	90.35	0.9810	0.1709	95.62
WANNGWL15	Haar-3 R (t-2), DB-2 ET (t-1), DB-2H (t-1)	3-15-1	0.9713	0.1951	94.33	0.9818	0.1718	95.57
WANNGWL16	Haar-3 R (t-2), DB-2 ET (t-1), DB-2H (t-1)	3-16-1	0.9714	0.1946	94.36	0.9813	0.1697	95.68
WANNGWL17	Haar-3 R (t-2), DB-2 ET (t-1), DB-2H (t-1)	3-17-1	0.9714	0.1946	94.36	0.9813	0.1697	95.68
WANNGWL18	Haar-3 R (t-2), DB-2 ET (t-1), DB-2H (t-1)	3-18-1	0.9711	0.1955	94.31	0.9804	0.1740	95.46
WANNGWL19	Haar-3 R (t-2), DB-2 ET (t-1), DB-2H (t-1)	3-19-1	0.9713	0.1949	94.34	0.9810	0.1708	95.63
WANNGWL20	Haar-3 R (t-2), DB-2 ET (t-1), DB-2H (t-1)	3-20-1	0.9711	0.1956	98.04	0.9804	0.1740	95.46



Figure 3. The WANN model structure.

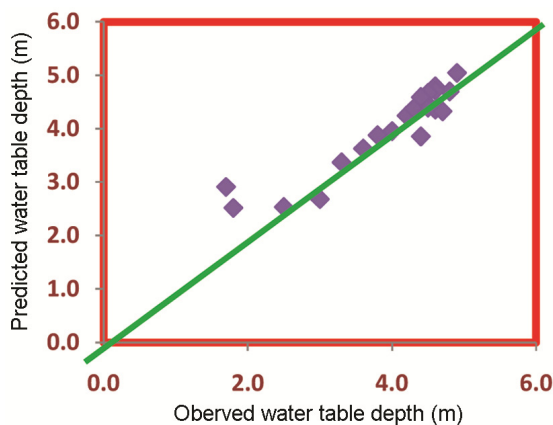


Figure 4. Scatter plot for the result of best ANN model during validation.

was similar for both evapotranspiration and water table depth signal, so, it could capture the signal features, especially peak points efficiently and led to comparatively good results.

The Haar wavelet has a pulsed shape (as shown in Figure 4) which is similar to the rainfall time series and helps in capturing the signal features and yield with moderately high efficiency. Hence, the Harr mother wavelet was chosen for decomposition of rainfall time series as suggested earlier²⁶. Rainfall time series was decomposed at different decomposition levels from 1 to 5. Decomposition level 3 was found to give better results. These disintegrated input signals were used as input to develop hybrid WANN model as shown in Figure 3.

Training of WANN model

Out of 58 months (July 2008 to April 2014) dataset, 56-month data set was available for analysis considering 2-month time lag for rainfall series. In the 56 month dataset, 35 sets (63%) were used for calibration (training), whereas 21 sets (37%) were used for validation. The number of hidden neurons was found by a trial and error method, starting with one hidden neuron and increasing up to 20 neurons. The log sigmoid and pure linear transfer functions were used for hidden and output layers respectively and the results of WANN model are given in Table 1.

Among the various WANN models, the WANNGWL10 model with WANN structure 3-10-1 was found best with highest correlation coefficient (0.9714 for calibration and 0.9813 for validation), highest model efficiency (94.36% for calibration and 95.68% for validation) and least RMSE (0.1946 m for calibration and 0.1695 m for validation). Even though there was not much difference in results among the structures from WANNGWL2 to

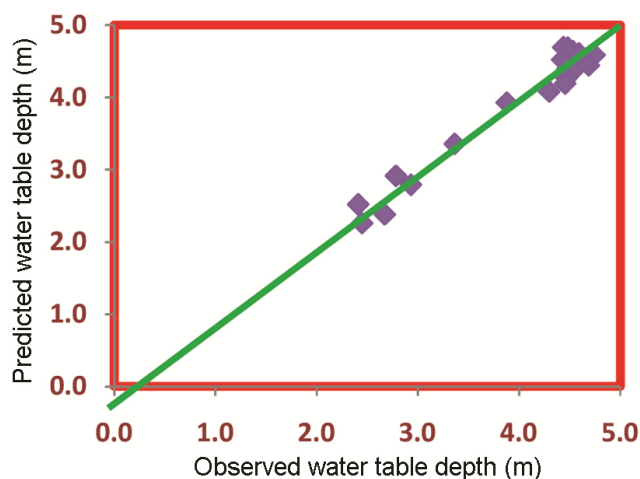


Figure 5. Scatter plot for the result of best WANN model during validation.

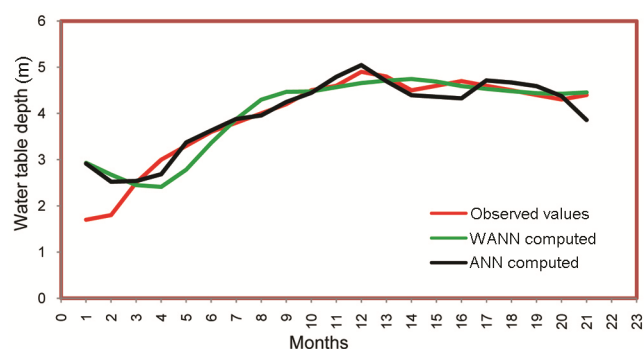


Figure 6. Observed, ANN and WANN computed monthly water table depths for validation period.

WANNGWL10, RMSE values were different and were used to select the significant model. Moreover the performance was increasing gradually; there was no fluctuation. Hence the model with WANN structure 3-10-1 was selected as the best WANN model.

The performance of best ANN and WANN model for prediction of water level depth at Roorkee during validation period was also analysed using scatter plots as shown in Figures 4 and 5 respectively, which clearly demonstrated the potential of the developed WANN models over ANN. The performance of the best ANN model and the best WANN model in terms of observed and predicted monthly groundwater table depths in the observation well during the validation period are shown in Figure 6, which clearly indicates that the WANN model predicted groundwater table depth closely matches with the observed groundwater table depth as compared to those simulated by the ANN model. The presented results bring out the superiority as well as potential applicability of the proposed WANN model for the forecast of monthly groundwater table fluctuation for Roorkee groundwater observation station operated and maintain by NIH.

Conclusion

The accurate groundwater depth fluctuation forecast is an important issue for sustainable development and management of regional water resources in the country. In view of the hydro-geological complexities involved in the forecast of groundwater depth by statistical, empirical or physically based models, the data-driven models are simple, comparatively data inexpensive as well as accurate. Therefore, in the present study, an attempt was made to apply a data-driven ANN and WANN models to verify the performance and their applicability to forecast monthly groundwater depth fluctuation using the observed data from groundwater observation well operated and maintained by NIH, Roorkee. The computed RMSE values of ANN and WANN model during validation were found to be 0.3648 m and 0.1695 m respectively, which shows a decrease in RMSE value by 0.1950 m when WANN was applied. Similarly, the computed model efficiencies of ANN and WANN model during validation were 84.65% and 95.68% indicating excellent improvement of model accuracy after applying WANN. These results indicate that the WANN model shows substantial improvement in the model performance as compared to ANN model results. Therefore, from the results of these study, it could be concluded that the performance of the proposed WANN model in the forecasting of the monthly groundwater depth fluctuations is substantially improved when the wavelet transform is combined with ANN model as compared to the groundwater depth forecasting results by ANN model. In addition, comparison of the time series plots and the scatter plots developed using the results of ANN and WANN model results showed that the water level depth values forecast using the WANN model were more precise and were very near to observed data as compared to those by the ANN model. Therefore, the proposed WANN model seems a promising tool for forecasting monthly groundwater depth fluctuations. However, the performance of the WANN model for forecasting of the daily groundwater depth fluctuation needs to be verified, which will be carried out in the near future.

1. French, M. N., Krajewski, W. F. and Cuykendall, R. R., Rainfall forecasting in space and time using a neural network. *J. Hydrol.*, 1992, **137**, 1–31.
2. Nayak, P. C., Satyaji Rao, Y. R. and Sudheer, K. P., Groundwater level forecasting in a shallow aquifer using artificial neural network approach. *Water Resour. Manage.*, 2006, **20**, 77–90.
3. Krishna, B., Satyaji Rao, Y. R. and Vijaya, T., Modelling groundwater levels in an urban coastal aquifer using artificial neural networks. *Hydrol. Process*, 2008, **22**, 1180–1188.
4. Nakhaei, M. and Saberi Nasr, A., A combined wavelet-artificial neural network model and its application to the prediction of groundwater level fluctuations. *J. Geope.*, 2012, **2(2)**, 77–91.
5. Vetrivel. N. and Elangovan. K., Prediction and forecasting of groundwater level fluctuation by ANN technique. *Int. J. Civil Eng. Technol.*, 2016, **7(5)**, 401–408.

6. Rhif, M., Abbes, A. B., Farah, I. R., Martinez, B. and Sang, Y., Wavelet transform application for/in non-stationary time-series analysis: a review. *Appl. Sci.*, 2019, **9**, 1345.
7. Zhou, H. C., Peng, Y. and Liang, G. H., The research of monthly discharge predictor-corrector model based on wavelet decomposition. *Water Resour. Manage.*, 2008, **22**, 217–227.
8. Nourani, V. and Parhizkar, M., Conjunction of SOM-based feature extraction method and hybrid wavelet-ANN approach for rainfall–runoff modeling. *J. Hydroinform.*, 2013, **15**(3), 829–848.
9. Grossmann, A. and Morlet, J., Decomposition of Hardy function into square integrable wavelets of constant shape. *J. Math. Anal.*, 1984, **15**(4), 723–736.
10. Adamowski, J. and Sun, K., Development of a coupled wavelet transform and neural network method for flow forecasting of non-perennial rivers in semi-arid watersheds. *J. Hydrol.*, 2010, **390** (1–2), 85–91.
11. Kisi, O., Neural networks and wavelet conjunction model for intermittent stream-flow forecasting. *J. Hydrol. Eng.*, 2009, **14**(8), 773–782.
12. Kisi, O., Neural network and wavelet conjunction model for modeling monthly level fluctuations in Turkey. *Hydrol. Process.*, 2009, **23**(14), 2081–2092.
13. Nourani, V., Kisi, O. and Komasi, M., Two hybrid artificial intelligence approaches for modeling rainfall–runoff process. *J. Hydrol.*, 2011, **402**(1–2), 41–59.
14. Maheswaran, R. and Khosa, R., Comparative study of different wavelets for hydrologic forecasting. *Comput. Geosci.*, 2012, **46**, 284–295.
15. Maheswaran, R. and Khosa, R. Wavelet-Volterra coupled model for monthly stream flow forecasting. *J. Hydrol.*, 2012, **450**, 320–335.
16. Sang, Y. F., A practical guide to discrete wavelet decomposition of hydrologic time series. *Water Resour. Manage.*, 2012, **26**(11), 3345–3365.
17. Tiwari, M. K. and Chatterjee, C., A new wavelet-bootstrap-ANN hybrid model for daily discharge forecasting. *J. Hydroinform.*, 2011, **13**(3), 500–519.
18. Bhabagrahi, S., Imtisenla, W., Bidyut, C. D. and Bhagwati, P. B., Standardization of reference evapotranspiration models for a sub humid valley rangeland in the Eastern Himalayas. *J. Irrig. Drain Eng.*, 2012, **138**, 880–895.
19. Fausett, L., *Fundamentals of Neural Networks*, Prentice Hall, Englewood Cliffs, NJ, 1994.
20. Maier, H. R. and Dandy, G. C., Neural networks for the prediction and forecasting of water resources variables: a review of modeling issues and applications. *Environ. Modell. Softw.*, 2000, **15**, 101–124.
21. Anctil, F., Perrin, C. and Andreassian, V., Impact of the length of observed records on the performance of ANN and of conceptual parsimonious rainfall-runoff forecasting models. *Environ. Modeling Software*, 2004, **19**(4), 357–368.
22. Porter, D. W., Gibbs, P. G., Jones, W. F., Huyakorn, P. S., Hamm, L. L. and Flach, G. P., Data fusion modeling for groundwater systems. *J. Contaminant Hydrol.*, 2000, **42**, 303–335.
23. Mallat, S., A theory for multiresolution signal decomposition: The wavelet representation. *IEEE Trans. Pattern Anal. Mach. Intell.*, 1989, **11**, 674–693.
24. Cannas, B., Fanni, A., See, L. and Sias, G., Data pre-processing for river flow forecasting using neural networks: wavelet transforms and data partitioning. *Phys. Chem. Earth.*, 2005, **31**, 1164–1171.
25. Chandrasekhar, E., Dimri, V. P. and Gadre, V. M., *Wavelets and Fractals in Earth System Sciences*, CRC Press, Taylor and Francis, UK, 2013.
26. Nourani, V., Komasi, M. and Mano, A., A multivariate ANN Wavelet approach for rainfall-runoff modeling. *Water Resour. Manage.*, 2009, **23**, 2877–2894.

Received 27 February 2019; accepted 7 July 2019

doi: 10.18520/cs/v117/i9/1475-1481